SAND2019-13955PE

# Strategy and Status for Bounding Open Room Closure Porosity/Permeability Response

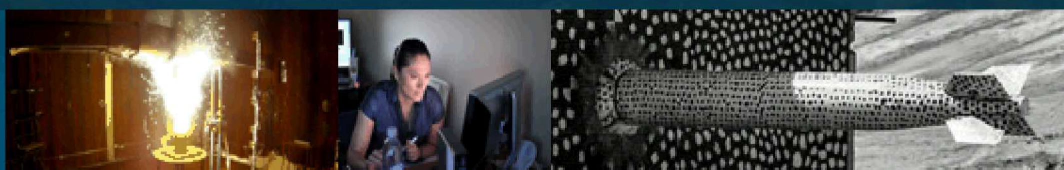

PRESENTED BY

Ed Matteo, Tom Dewers, Chven Mitchell, Rob Lander, and Linda Bonell

# Overview

-Overall conceptual approach

-Brief review of literature in this area

-GEOCOSM -Some related work done in sandstone diagenesis

-Status of SNL-GEOCOSM collaboration

-Proposed experimental work at UNM

-Needs for intact WIPP Salt moving forward

# Conceptual Strategy

1) Create multiple realizations of a polydisperse ("poorly sorted") random packing arrangement

- Main variables to vary
  - degree of polydispersity, i.e., size distribution function
    - Why? Because we're not sure how varied the rubble pile will be
  - The actual random packing arrangement
    - Why? Because we're not sure if how/when the rubble falls makes a difference, or how significant that difference might be on the ultimate permeability

2) Use CFD to evaluate flow through each packing arrangement

# Brief Overview o Literature

Key Points:

- Mode of construction
  - Sequential Deposition results in lower porosity than Monte Carlo
  - However, transport depends only on porosity
- Random and homogenous packing

PHYSICAL REVIEW E VOLUME 55, NUMBER 2 FEBRUARY 1997

**Geometrical and transport properties of random packings of spheres and aspherical particles**

D. Coelho,[1] J.-F. Thovert,[1] and P. M. Adler[2]

[1]*Laboratoire des Phénomènes de Transport dans les Mélanges (LPTM), SP2MI, Bd 3, Téléport 2, F-86960 Futuroscope, France*

[2]*IPGP, tour 24, 4, Place Jussieu, 75252 Paris Cedex 05, France*

(Received 7 March 1996; revised manuscript received 30 September 1996)

Random packings of grains of arbitrary shape are built with an algorithm that is mostly applied to spheres, ellipsoids, cylinders, and parallelepipeds. A systematic account of the main geometrical properties such as the porosity, the reduced specific area, etc. is given. The conductivity, the permeability, and the dispersion are also systematically determined and they are shown not to depend upon their mode of construction. [S1063-651X(97)13802-8]

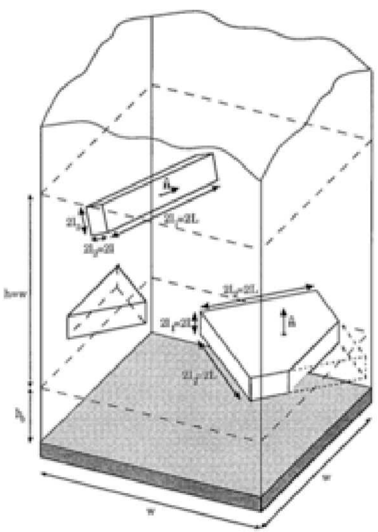


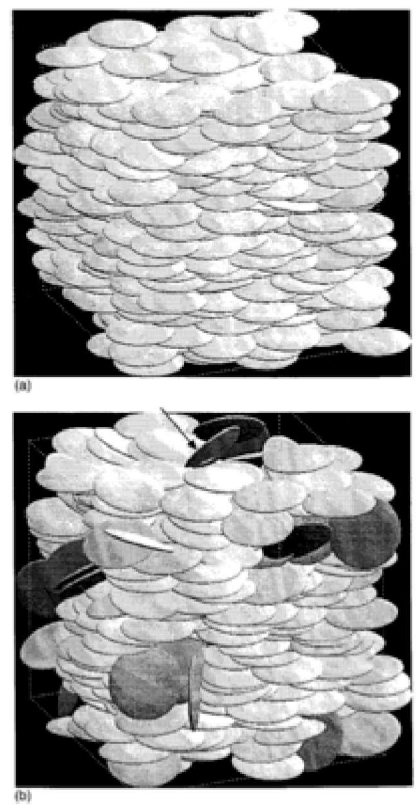


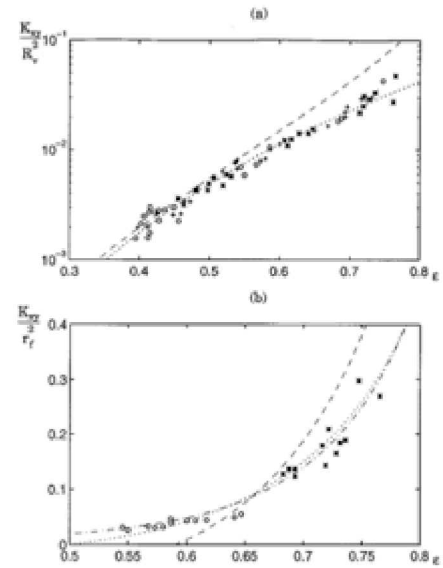


FIG. 15. Permeability as function of porosity. (a) $K_{xy}/R_v^2$ of random beds of ellipsoids (○), cylinders (+), and parallelepipeds (*) vs the porosity $\epsilon$. The dot is the measurement of Thiess-Weesie *et al.* [34]. The broken line is Eq. (34c) with $k/\Psi^2=10$; the dotted line is the least square fit Eq. (41). (b) The permeability $K_{xy}/r_f^2$ of random beds of prolate particles with $L/l=5$ (○) and 10 (*) vs the porosity $\epsilon$. The broken line is Eq. (37) with $k_4=6.1$ and $k_5=0.64$. The dotted line is Eq. (37) with $k_4=12.6$ and $k_5=0.707$. The dashed line is Eq. (38).

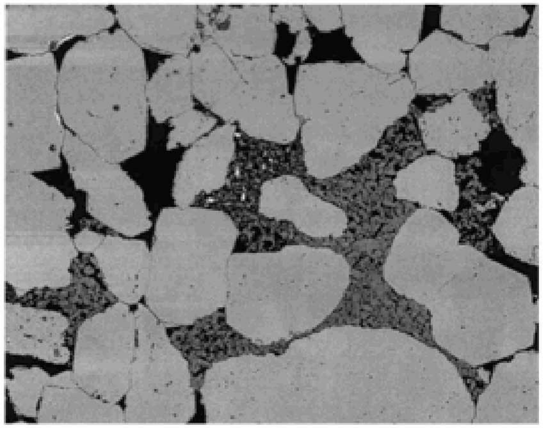

*Figure 1.* BSE image of a thin section from a North Sea reservoir sandstone. The pore space is black, solid (quartz/feldspar) is light grey, and clay is dark grey.

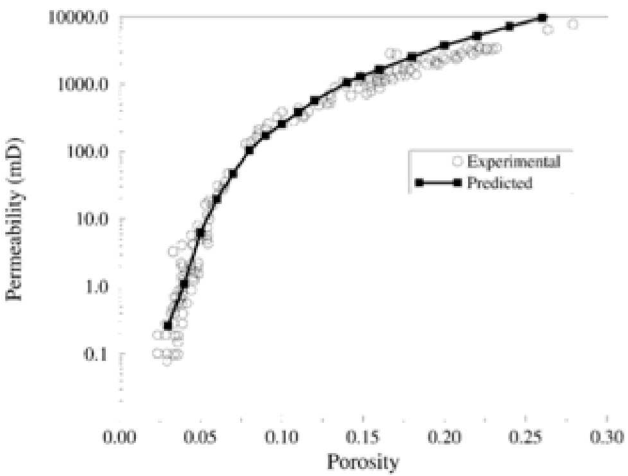


*Figure 13.* Comparison between measured and computed (directionally averaged) permeabilities of Fontainebleau sandstones.

*Transport in Porous Media* **46:** 311–343, 2002.




# Process Based Reconstruction of Sandstones and Prediction of Transport Properties

PÅL-ERIC ØREN and STIG BAKKE
*Statoil Research Centre, N-7005 Trondheim, Norway*

**Abstract.** We present a process based method for reconstructing the full three-dimensional microstructure of sandstones. The method utilizes petrographical information obtained from two-dimensional thin sections to stochastically model the results of the main sandstone forming processes – sedimentation, compaction, and diagenesis. We apply the method to generate Fontainebleau sandstone and compare quantitatively the reconstructed microstructure with microtomographic images of the actual sandstone. The comparison shows that the process based reconstruction reproduces adequately important intrinsic properties of the actual sandstone, such as the degree of connectivity, the specific internal surface, and the two-point correlation function. A statistical reconstruction of Fontainebleau sandstone that matches the porosity and two-point correlation function of the microtomography data differs strongly from the actual sandstone in its connectivity properties. Transport properties of the samples are determined by solving numerically the local equations governing the transport. Computed permeabilities and formation factors of process based reconstructions of Fontainebleau sandstone compare well with experimental measurements over a wide range of porosity.

**Key words:** 3D reconstruction, microstructure, Fontainebleau sandstone, percolation, permeability, formation factor.

PHYSICAL REVIEW E **80**, 021304 (2009)

# Numerical study of the effects of particle shape and polydispersity on permeability

Xavier Garcia,[1,*] Lateef T. Akanji,[1,†] Martin J. Blunt,[1,‡] Stephan K. Matthai,[2,§] and John Paul Latham[1,‖]
[1]*Department of Earth Science and Engineering, Imperial College London, SW72AZ London, United Kingdom*
[2]*School of Petroleum Engineering, Montanuniversität, Max-Tendler-Strasse, A-8700, Leoben, Austria*
(Received 11 May 2009; published 26 August 2009)

We study through numerical simulations the dependence of the hydraulic permeability of granular materials on the particle shape and the grain size distribution. Several models of sand are constructed by simulating the settling under gravity of the grains; the friction coefficient is varied to construct packs of different porosity. The size distribution and shapes of the grains mimic real sands. Fluid flow is simulated in the resulting packs using a finite element method and the permeability of the packs is successfully compared with available experimental data. Packs of nonspherical particles are less permeable than sphere packs of the same porosity. Our results indicate that the details of grain shape and size distribution have only a small effect on the permeabilty of the systems studied.

DOI: 10.1103/PhysRevE.80.021304 PACS number(s): 45.70.−n, 91.60.Np, 47.56.+r, 47.11.−j

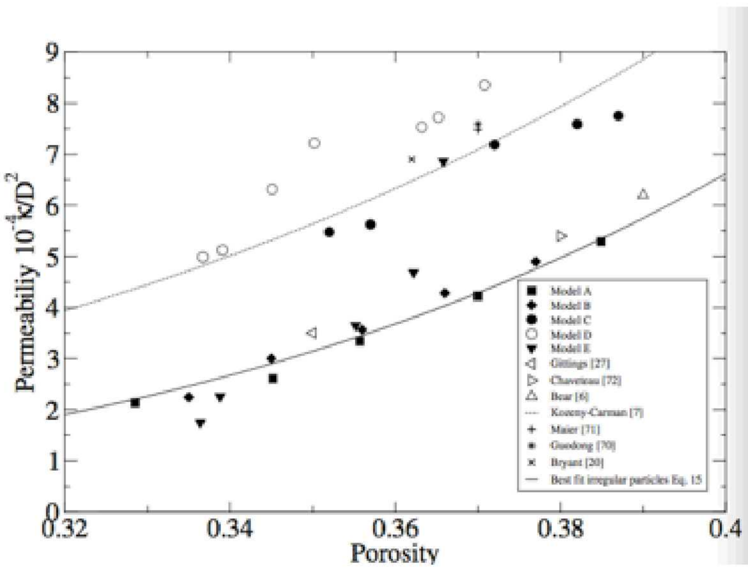


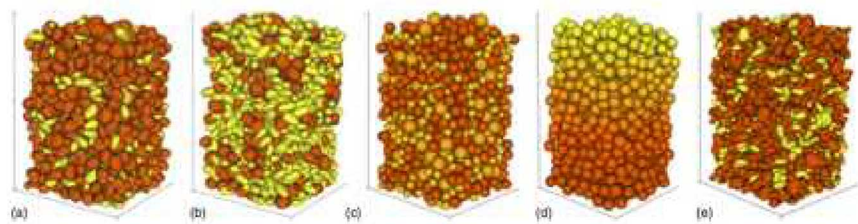


FIG. 4. (Color online) *A*: model *A* of a relatively homogeneous sand with semispherical grains. *B*: model *B*, as the previous model but a large number of grains were replaced by elongated grains (light colors). *C*: model *C*, spheres with the same size distribution as in *A*, *B*. *D*: single size spheres. *E*: more heterogeneous sample constructed with a mixture of irregular shapes.

Journal of Computational Physics 229 (2010) 3295–3315

Contents lists available at ScienceDirect

Journal of Computational Physics

journal homepage: www.elsevier.com/locate/jcp

# Using level sets for creating virtual random packs of non-spherical convex shapes

D. Shane Stafford[a], Thomas L. Jackson[b,*]

[a] Theoretical and Applied Mechanics, University of Illinois at Urbana-Champaign, United States
[b] Center for Simulation of Advanced Rockets at the University of Illinois at Urbana-Champaign, United States

ARTICLE INFO

*Article history:*
Received 16 January 2009
Received in revised form 22 November 2009
Accepted 5 January 2010
Available online 20 January 2010

*Keywords:*
Level sets
Random packs
Energetic materials
Sphere packing
Solid rockets
Propellants
Heterogeneous material
Porous material

ABSTRACT

Random packs of spheres have been used to model heterogeneous and porous material morphologies during simulations of physical processes such as burning of coal char, convective burning in porous explosives, and regression of solid rocket propellant. Sphere packs have also been used to predict thermo-mechanical properties, permeability, packing density, and dissolution characteristics of various materials. In this work, we have extended the Lubachevsky–Stillinger (LS) sphere packing algorithm to create polydisperse packs of non-spherical shapes for modeling heterogeneity in complex energetic materials such as HMX and pressed gun propellants. In the method, we represent the various particle shapes using level sets. The LS framework requires estimates of inter-particle collision times, and we predict these times by numerically solving a minimization problem. We have obtained results for dense random packs of various convex shapes such as cylinders, spherocylinders, and polyhedra, and we show results with these various particles packed together in a single pack to high packing fraction.



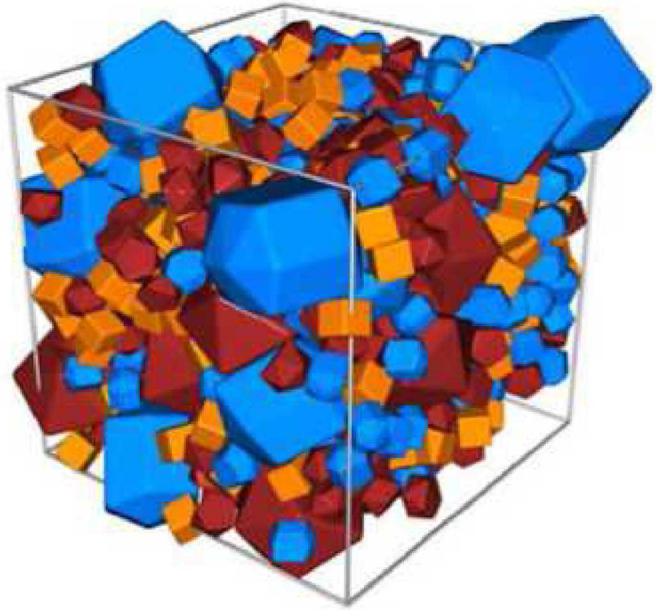

# Deposition is currently done using NVIDIA's PhysX compute engine, created for gaming and animation.

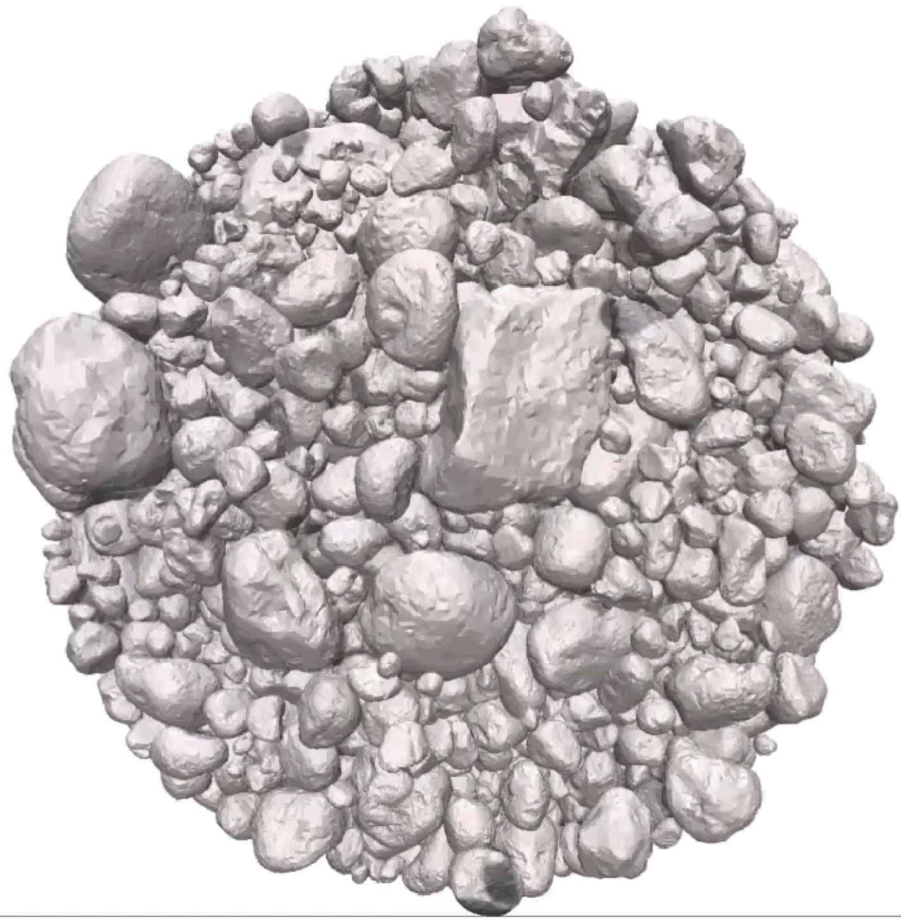

# Compaction vs. Ductile Grain Abundance

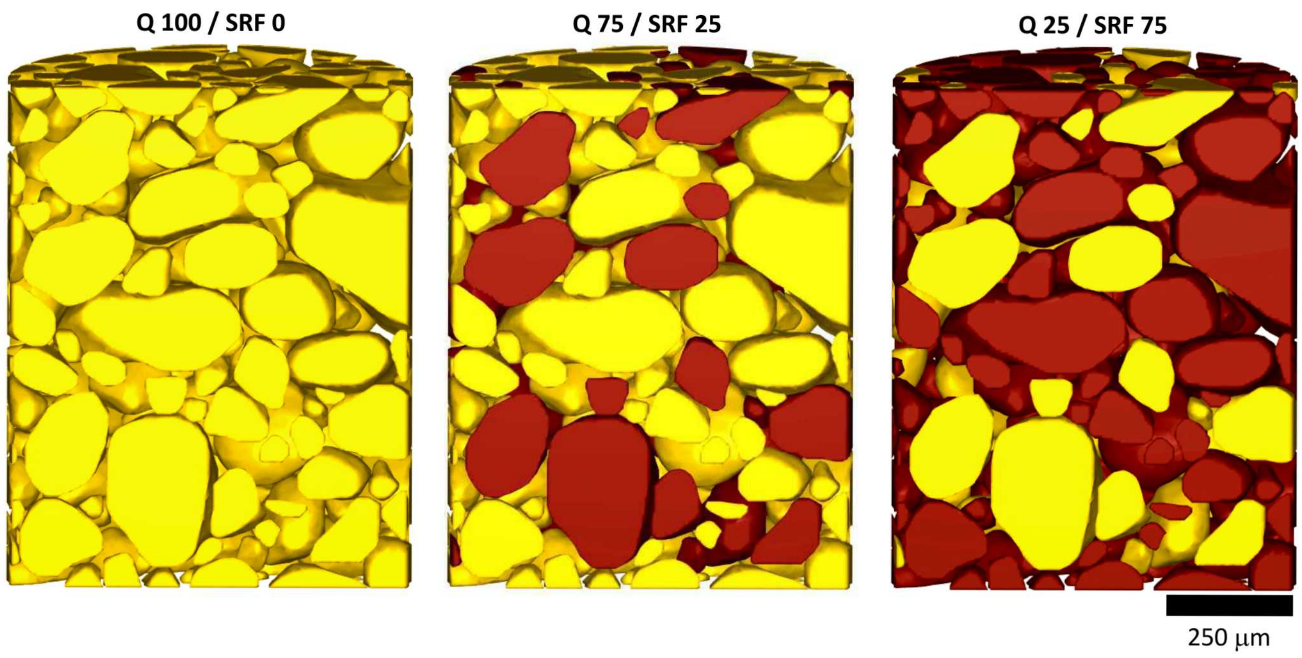

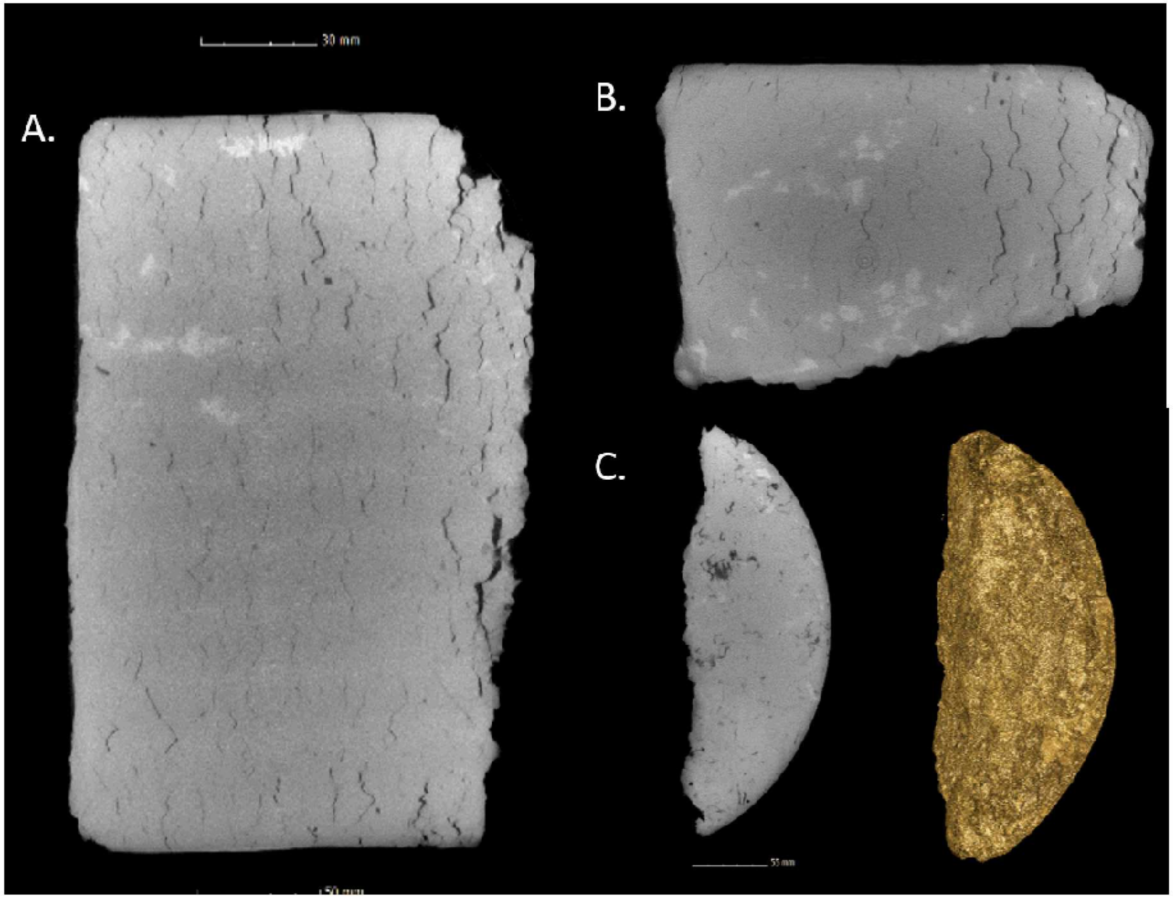
30 mm
A.
B.
C.

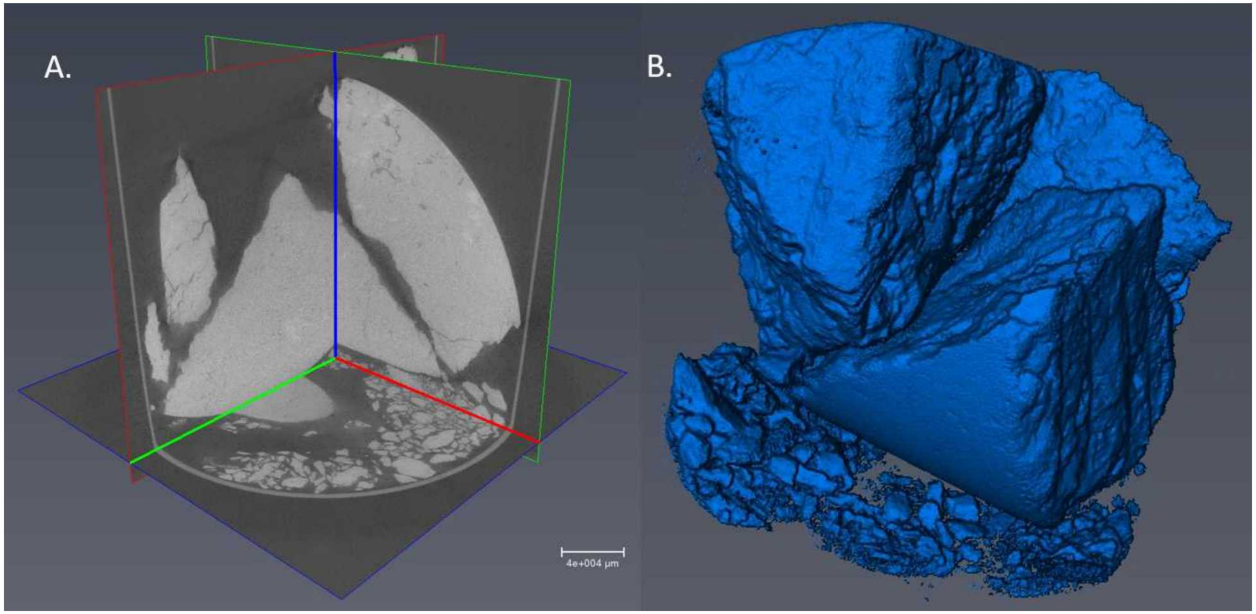
A.
4e+004 µm
B.

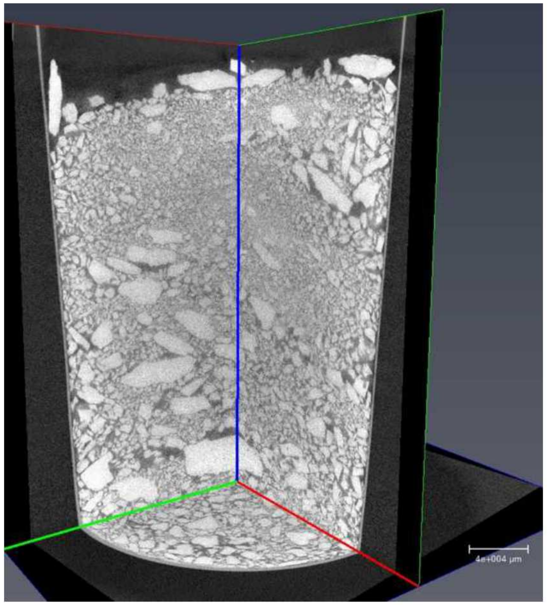
4e+004 µm

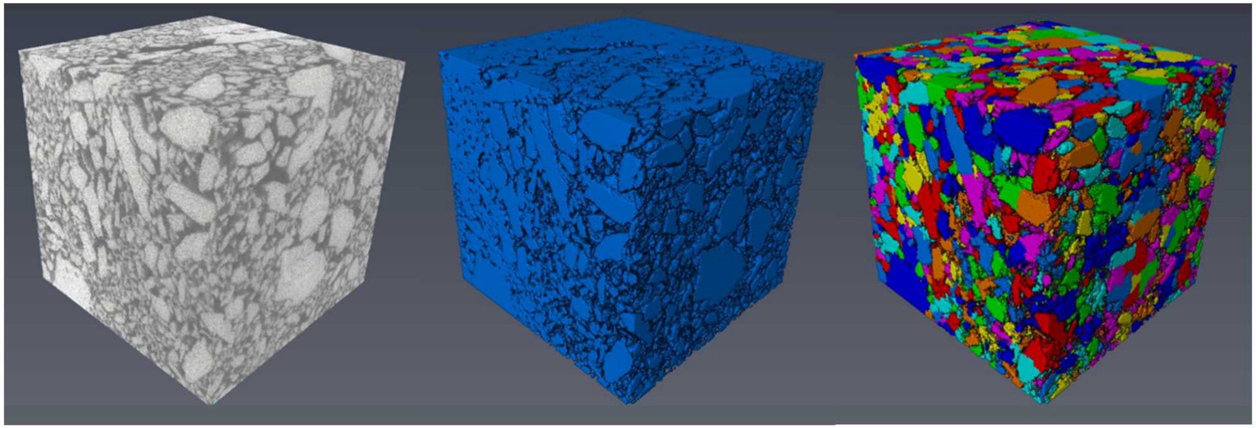

Original Sample (grains appear light grey)

Segmented (grains appear solid blue)

Separated Grains – note large grains are divided by choice of current algorithm

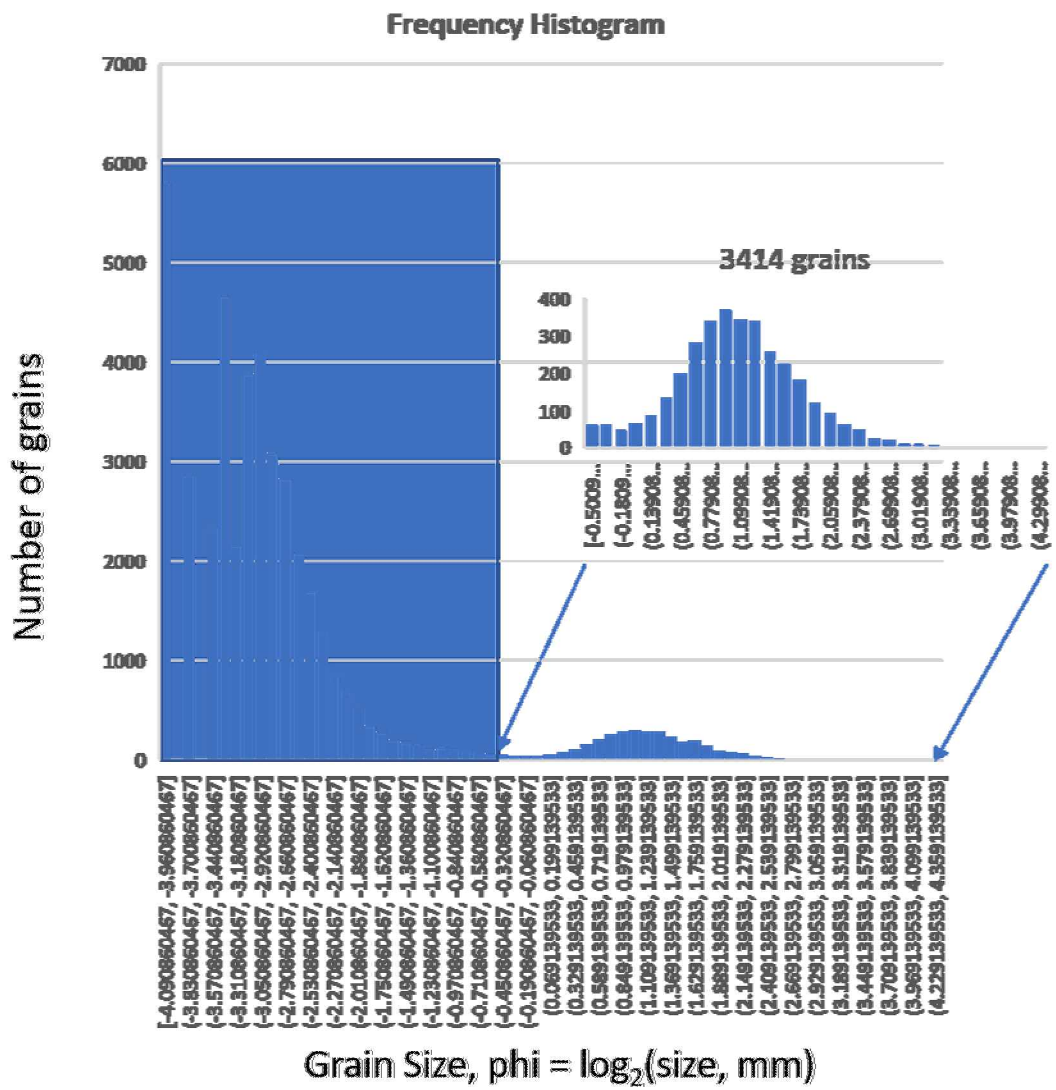

Frequency Histogram
Number of grains
7000
6000
5000
4000
3000
2000
1000
0
3414 grains
400
300
200
100
0
[-0.5009...
(-0.1809...
(0.13908...
(0.45908...
(0.77908...
(1.09908...
(1.41908...
(1.73908...
(2.05908...
(2.37908...
(2.69908...
(3.01908...
(3.33908...
(3.65908...
(3.97908...
(4.29908...
[-4.090860467, -3.960860467]
(-3.830860467, -3.700860467]
(-3.570860467, -3.440860467]
(-3.310860467, -3.180860467]
(-3.050860467, -2.920860467]
(-2.790860467, -2.660860467]
(-2.530860467, -2.400860467]
(-2.270860467, -2.140860467]
(-2.010860467, -1.880860467]
(-1.750860467, -1.620860467]
(-1.490860467, -1.360860467]
(-1.230860467, -1.100860467]
(-0.970860467, -0.840860467]
(-0.710860467, -0.580860467]
(-0.450860467, -0.320860467]
(-0.190860467, -0.060860467]
(0.069139533, 0.199139533]
(0.329139533, 0.459139533]
(0.589139533, 0.719139533]
(0.849139533, 0.979139533]
(1.109139533, 1.239139533]
(1.369139533, 1.499139533]
(1.629139533, 1.759139533]
(1.889139533, 2.019139533]
(2.149139533, 2.279139533]
(2.409139533, 2.539139533]
(2.669139533, 2.799139533]
(2.929139533, 3.059139533]
(3.189139533, 3.319139533]
(3.449139533, 3.579139533]
(3.709139533, 3.839139533]
(3.969139533, 4.099139533]
(4.229139533, 4.359139533]
Grain Size, phi = log2(size, mm)

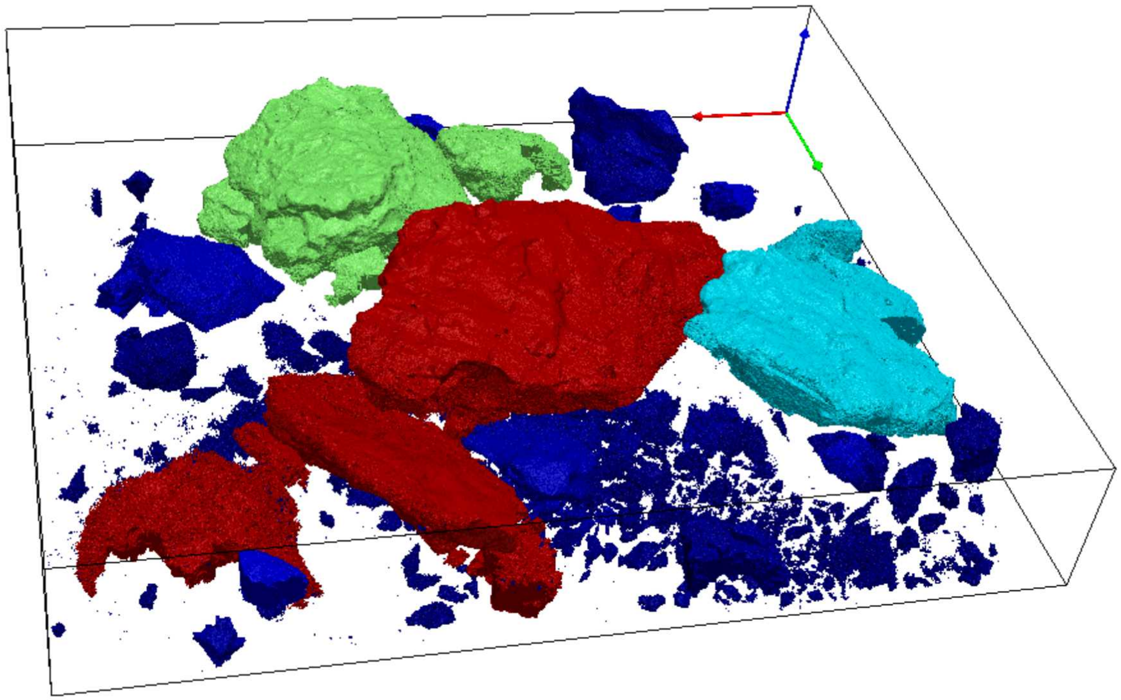

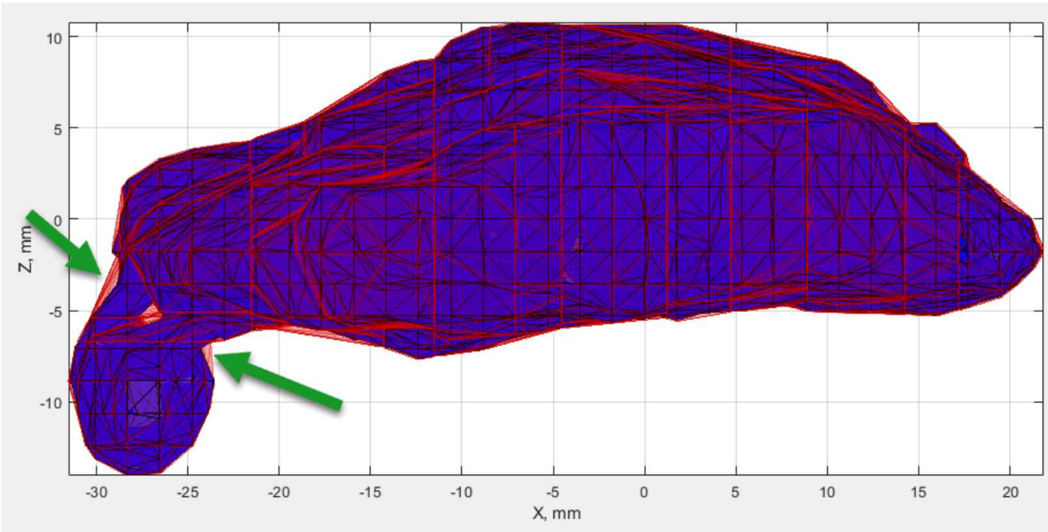
Z, mm
10
5
0
-5
-10
-30
-25
-20
-15
-10
-5
0
5
10
15
20
X, mm

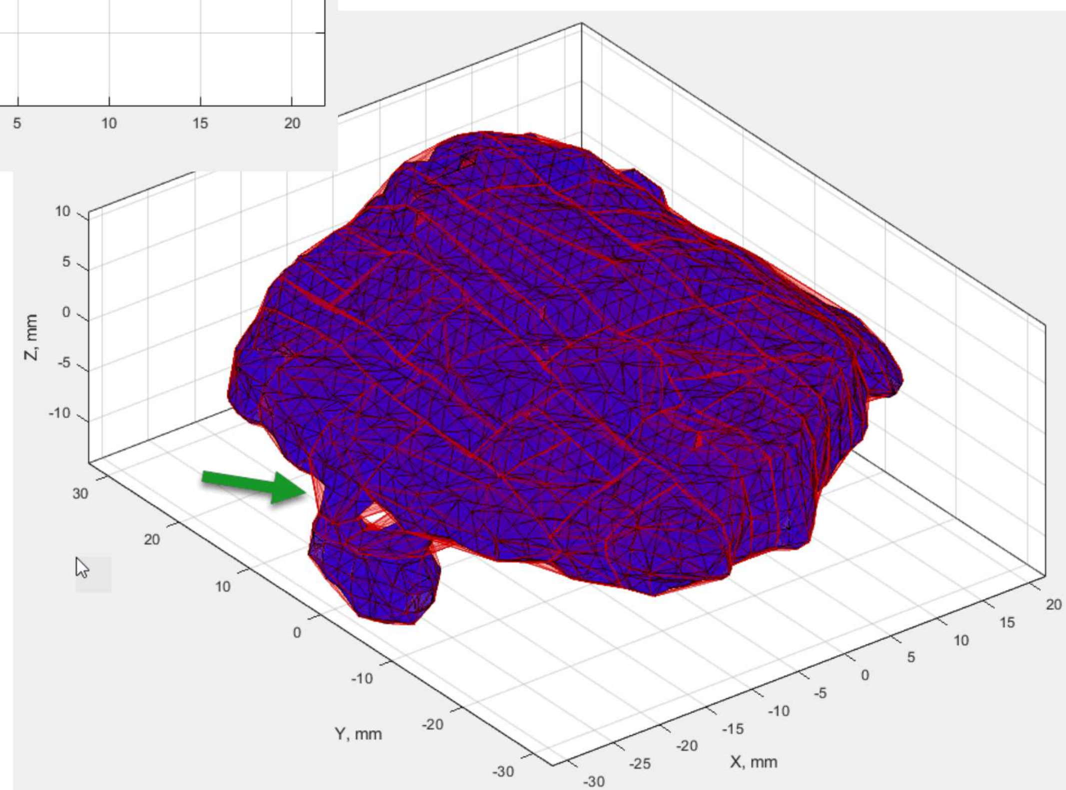
Z, mm
10
5
0
-5
-10
Y, mm
30
20
10
0
-10
-20
-30
X, mm
-30
-25
-20
-15
-10
-5
0
5
10
15
20

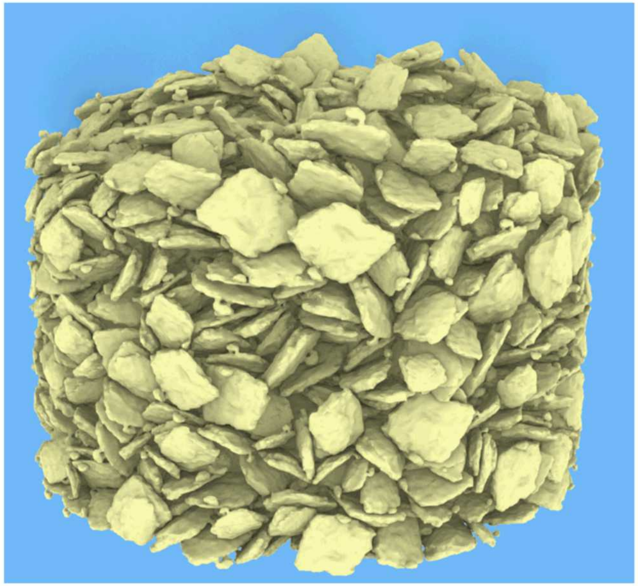

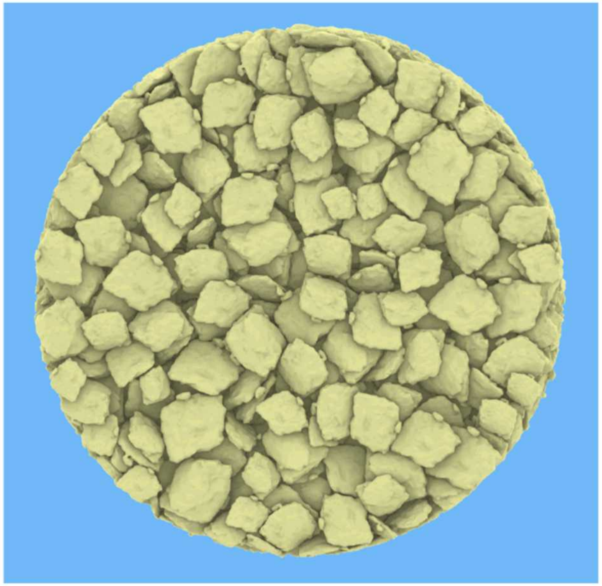

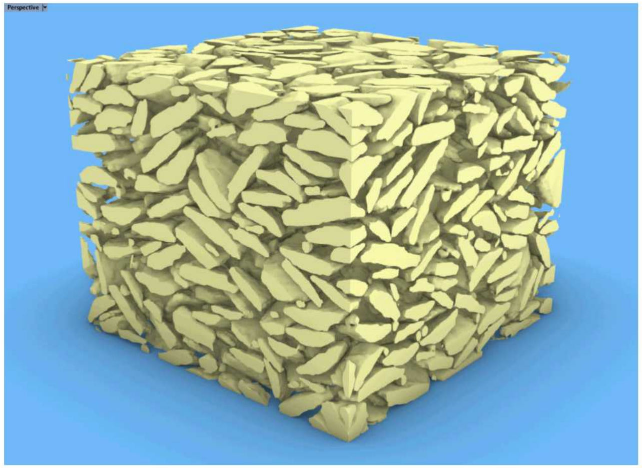
Perspective

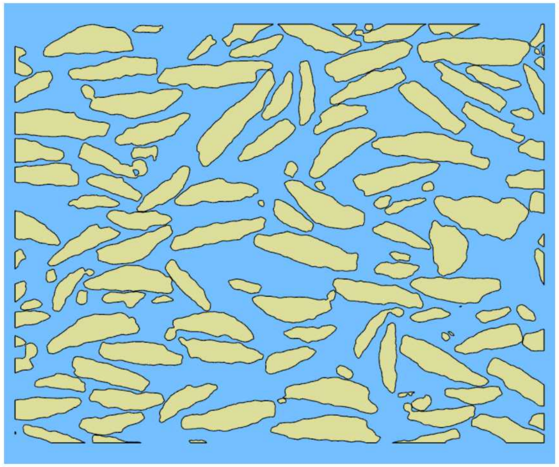

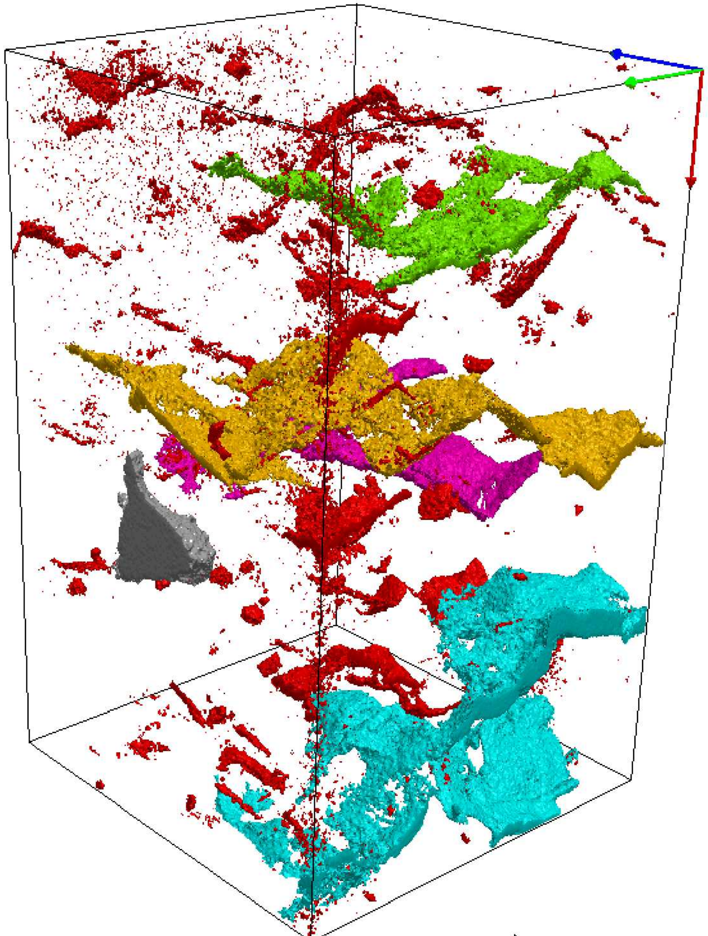

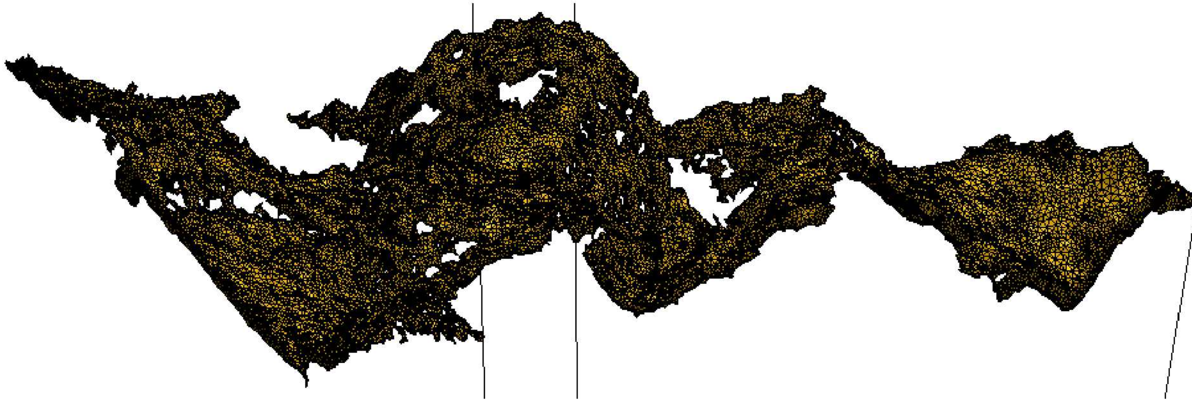

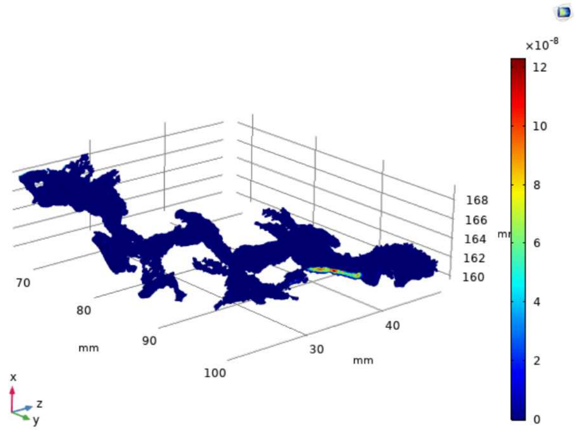


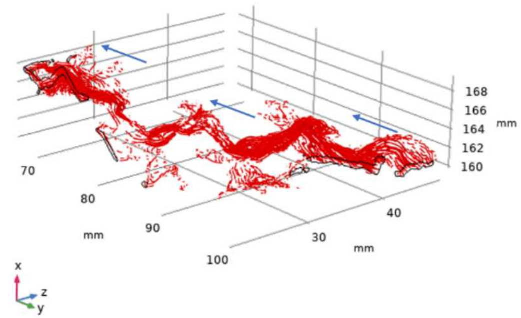


1. Characterization of rubble size and shape using X-ray micro-computed tomography
2. Image analysis to include solid segmentation and grain separation, using a variety of filters and watershed methods.
3. Creation of grain size distributions of rubble piles
4. Creation of grain surface meshes extracted from the separated particles, using the distribution as a guide.
5. Cyberstone modeling of rubble consolidation, extracting representative shapes and sizes using the provided STL files and the resulting volume distribution as a guide.
6. CFD modeling of gas transport in the consolidating rubble piles from the Cyberstone results.

Geomechanics Laboratory

# Intermediate scale testing of the permeability and porosity of rock salt after roof fall

Objective: Measure the range of permeabilities and porosities of salt fall material until it behaves as a mass of consolidating granular salt in the room. These data will be used to validate numerical approaches to modeling room behavior in response to roof fall.

## Conceptual model of room condition after fall with time

**Time**

**After fall**

Room closure is not impeded by roof fall material in room. Porosity >50%. Permeability very large and governed by large connected voids in room.

**Densification from particle rearrangement**

Salt in room densifies largely by particle rearrangement and some particle breakage. Fall material offers very little but increasing resistance with closure. Porosity ~ 50% to 30%. Permeability is largely unknown but may achieve a value that affects performance/risk assessments.

**Densification from consolidation**

Salt in room from fall behaves as mass of consolidating salt – there is existing data on mechanical and hydrologic properties of salt in this state.

Study is directed at measuring permeability and porosity of room material under these conditions.

# Test configuration

**Porosity system**
Connect reservoir of known volume and pressure to unknown pore volume of salt and allow to equilibrate. Porosity interpreted from equilibrium pressure.

**Permeability system**
Vacuum induces flow through salt. Pressure drop (P) and flow rate (Q) measured to interpret permeability.

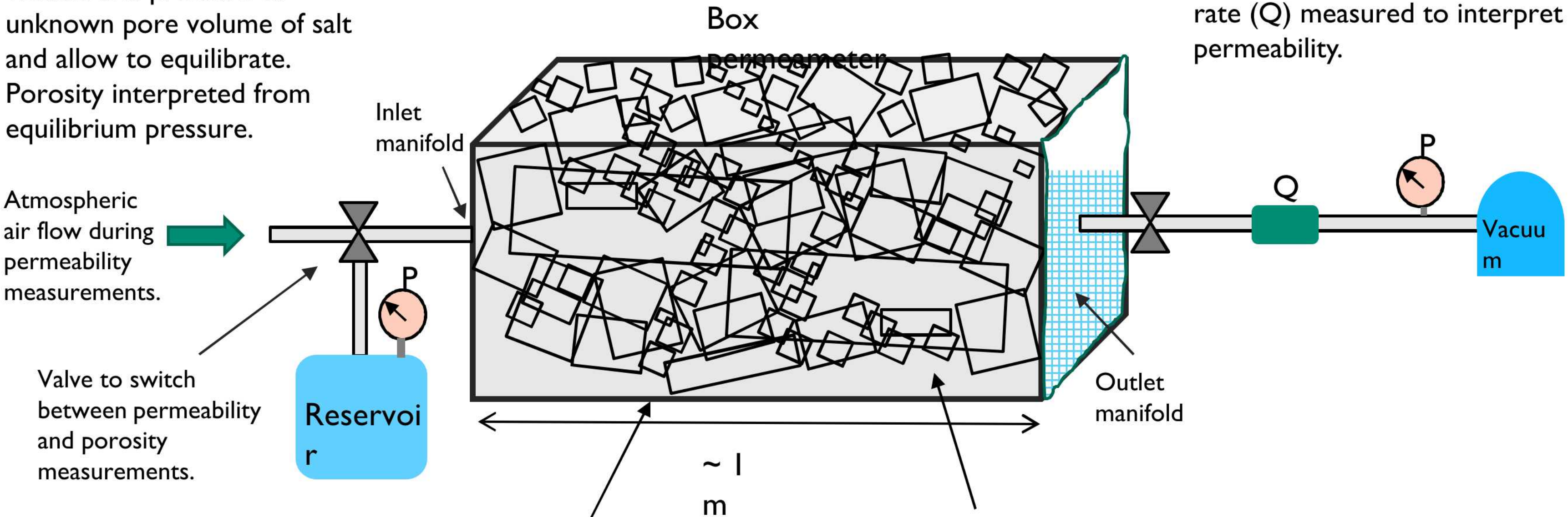


Box is portable. Permeability and porosity measurement systems can be disconnected.

***Salt particles contained within plastic liner that serves as jacket for vacuum permeability and porosity measurements.***

Geomechanics Laboratory

# Test sequence

1

Create mixtures of salt based on expected range of particle sizes.

2

Place salt of known mass in box permeameter. Measure permeability and porosity.

3

Densify material in box with large-scale vibratory table. Measure permeability and porosity.

Additional test options:

CT scan box and contents to confirm porosity measurements and reveal details about pore network.

Apply load via large-scale actuator to induce particle breakage and additional rearrangement.

Geomechanics Laboratory

# Expected results